

## Supplementary Information

### **EPR Spectroscopy Reveals Different Cu(II) Coordination in APP<sub>142–172</sub> and APP<sub>145–170</sub> Peptide Fragments of Amyloid Precursor Protein**

Liya Xu<sup>a, b</sup>, Jian Kuang<sup>b</sup>, Aokun Liu<sup>c</sup>, Lianghuan Liao<sup>c</sup>, Lu Yu<sup>\*b</sup> and Changlin Tian<sup>\*a, c</sup>

---

<sup>a</sup>High Magnetic Field Laboratory, Hefei Institutes of Physical Science, Chinese Academy of Sciences, Hefei, Anhui 230031, China.

<sup>b</sup>Department of Environmental Science and Engineering, University of Science and Technology of China, Hefei, Anhui 230026, China

<sup>c</sup>School of Chemistry and Chemical Engineering, Zhang jiang Institute for Advanced Sciences, Shanghai Jiao Tong University, Shanghai 201203, China.

#### **Corresponding Author**

\*E-mail: [luyuesr@ustc.edu.cn](mailto:luyuesr@ustc.edu.cn)

[cltian@sjtu.edu.cn](mailto:cltian@sjtu.edu.cn)

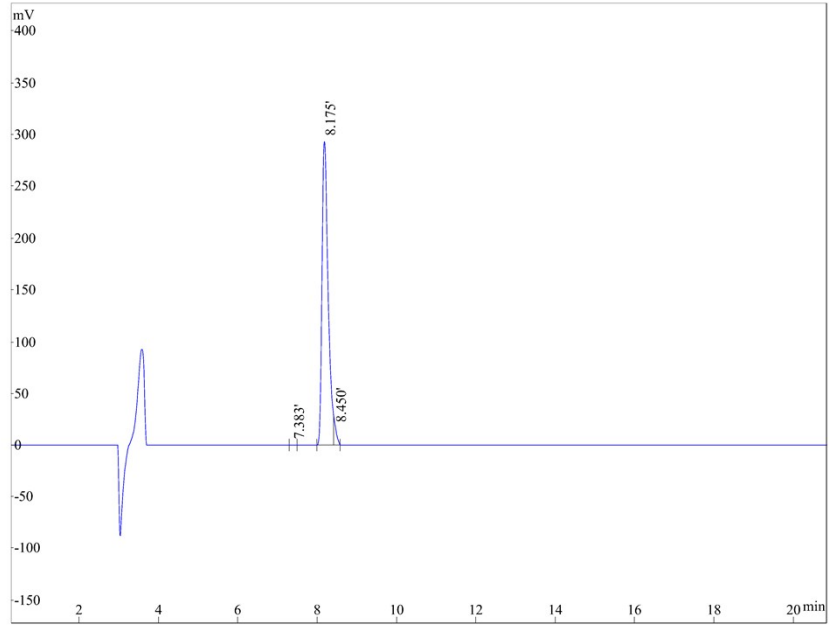


**Fig. S1** RP-HPLC chromatogram of APP<sub>142-172</sub>. Chromatography was performed on a C18 column (4.6 × 250 mm, 5 μm) using a linear gradient of acetonitrile/water containing 0.1% TFA, monitored at 220 nm. The peptide eluted as a major peak at 8.18 min with a purity of 96.8%.

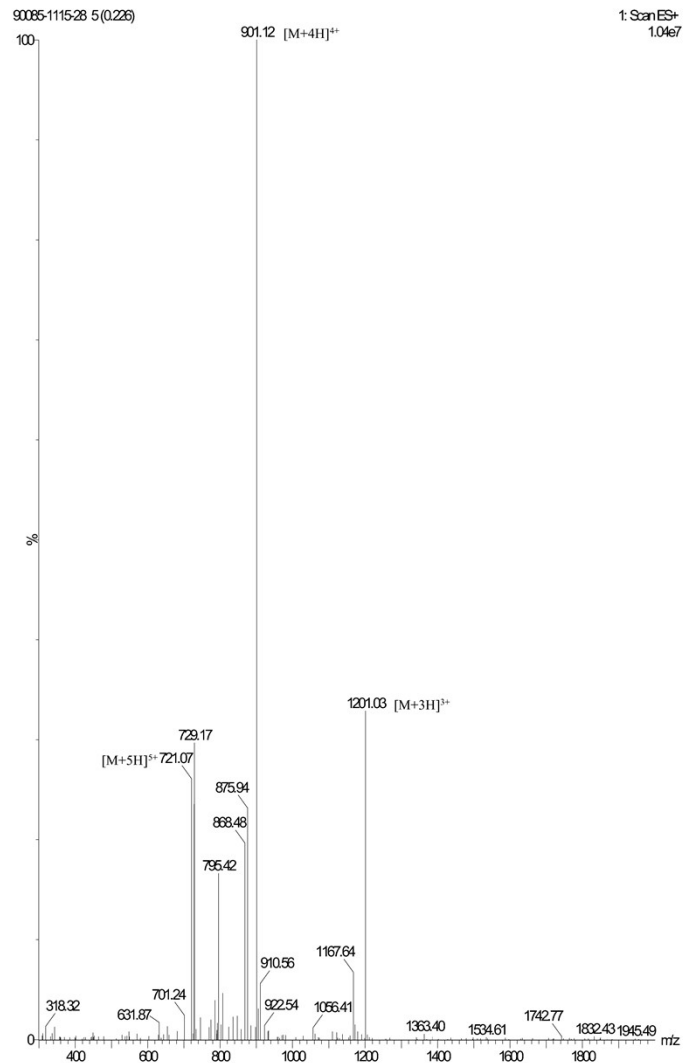


**Fig. S2** ESI-MS spectrum of peptide APP<sub>142-172</sub>. The observed multiply charged ions are consistent with the calculated molecular weight of the peptide (3599.0 Da).

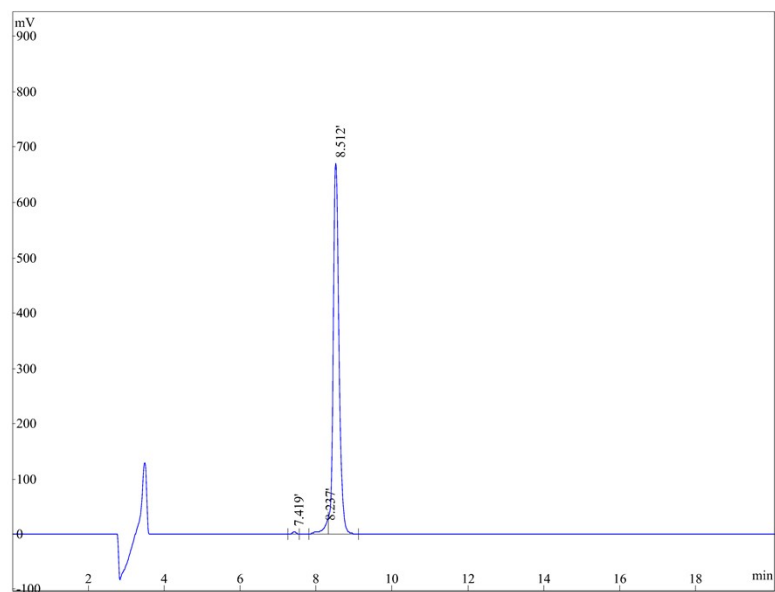


**Fig. S3** RP-HPLC chromatogram of APP<sub>145-170</sub>. Analysis was carried out on a C18 column with acetonitrile/water (0.1% TFA) as the mobile phase and UV detection at 220 nm. The main peak eluted at 8.51 min, corresponding to a purity of 95.6%.

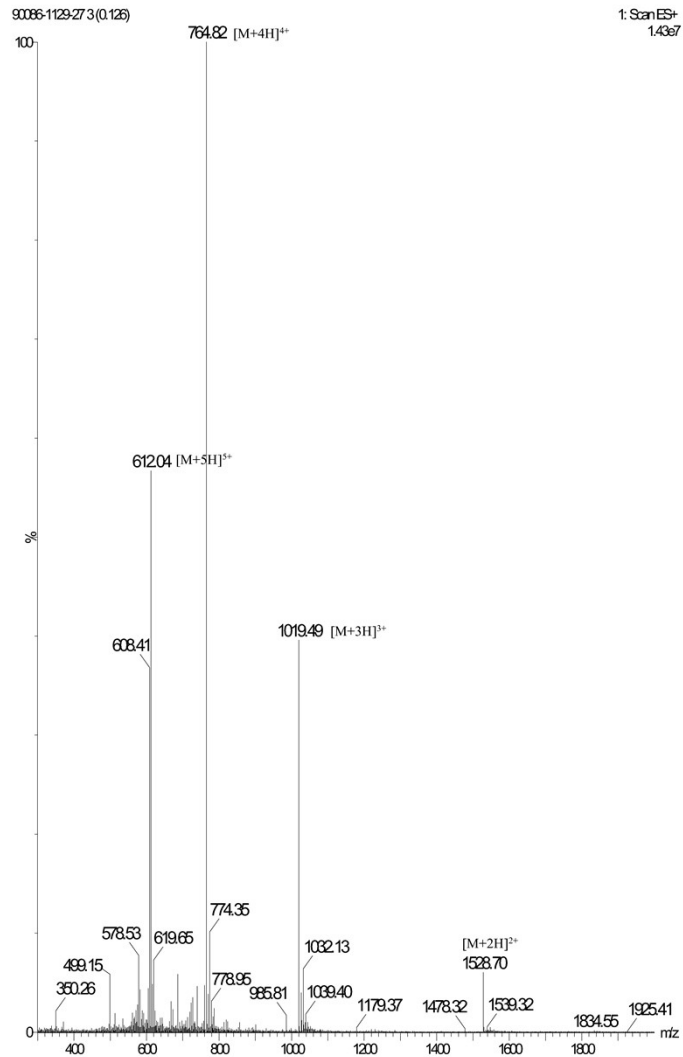


**Fig. S4** ESI-MS spectrum of peptide APP<sub>145-170</sub>. The experimental mass spectrum shows the expected charge-state distribution, confirming the molecular weight of the peptide (3055.4 Da).

Parameter	Cu(II)–APP <sub>142–172</sub>	Cu(II)–APP <sub>145–170</sub>
<b>g<sub>  </sub></b>	2.2725	2.2725
		2.1850
<b>g<sub>⊥</sub></b>	2.0553	2.0553
		2.0350
<b>A<sub>  </sub> (MHz)</b>	515	515
		600
<b>A<sub>⊥</sub> (MHz)</b>	35	35
		80
<b>g-strain(x/y/z)</b>	0.01/0.01/0.03	0.01/0.01/0.03
		0.01/0.01/0.03
<b>A-strain(x/y/z)</b>	10/10/90	10/10/90
		20/20/80
<b>g-AstrainCorr</b>	-1	-1
		-1
<b>Proportion</b>	1	0.4
		0.6
<b>f = g<sub>  </sub> / A<sub>  </sub> (cm)</b>	132.12	132.12
		109.25

**Table S1** Summary of simulation parameters obtained from EasySpin fitting of the EPR spectra. The ratio of  $g_{||}/A_{||}$ , denoted as  $f$ , can be considered as a measure of structural distortion and deviation from ideal geometry. The  $f$  value in the range of 110–120 cm is characteristic for Cu(II) centers with planar geometry, whereas its increase to approximately 150 cm indicates a slight to moderate distortion from planar symmetry.

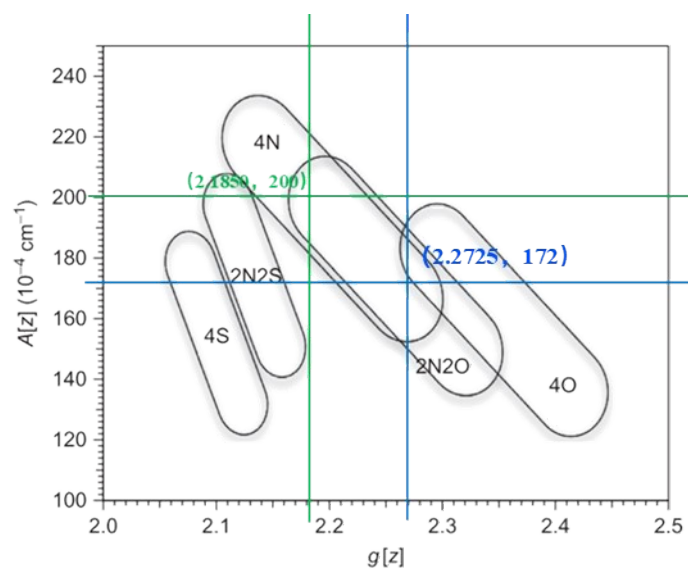


**Fig. S5** Peisach-Blumberg correlation plot of the copper(II) EPR parameters,  $g_{||}$  versus  $A_{||}$ . The blue traces correspond to component I, whose parameters fall within the  $N_2O_2$  region, indicating a mixed nitrogen-oxygen coordination sphere. The green traces represent component II, located near the 4N region, consistent with a nitrogen-rich ligand environment.

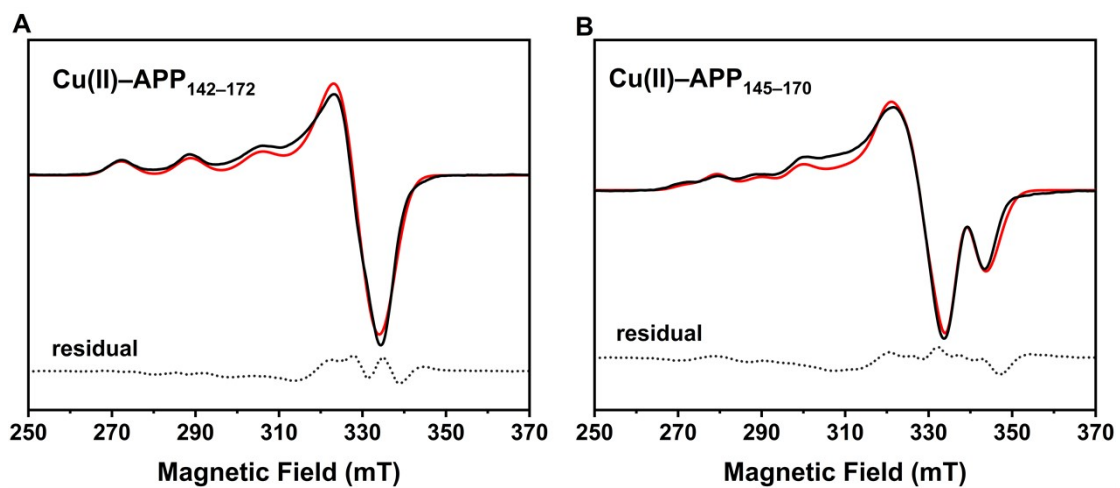


**Fig. S6** Residual spectra (Experimental spectra subtracted by Simulated spectra) for (A) Cu(II)-APP<sub>142-172</sub> and (B) Cu(II)-APP<sub>145-170</sub>, demonstrating the quality of the fits shown in Fig. 1.

pH	Cu(II)–APP <sub>142–172</sub>		Cu(II)–APP <sub>145–170</sub>	
	$g_{II}$	$A_{II} (10^{-4} \text{ cm}^{-1})$	$g_{II}$	$A_{II} (10^{-4} \text{ cm}^{-1})$
5.0	2.407	135	2.406	137
6.0	2.261	182	2.268	182
			2.171	213
7.0	2.260	184	2.258	181
			2.177	209
8.0	2.264	177	2.275	183
			2.182	207
9.0	2.261	179	2.279	185
			2.180	207
10.0	2.263	179	2.183	204

**Table. S2** pH-dependent EPR parameters ( $g_{II}$  and  $A_{II}$ ) for Cu(II)–APP<sub>142–172</sub> and Cu(II)–APP<sub>145–170</sub> complexes. For Cu(II)–APP<sub>145–170</sub>, values for both Component I and II are listed where applicable.

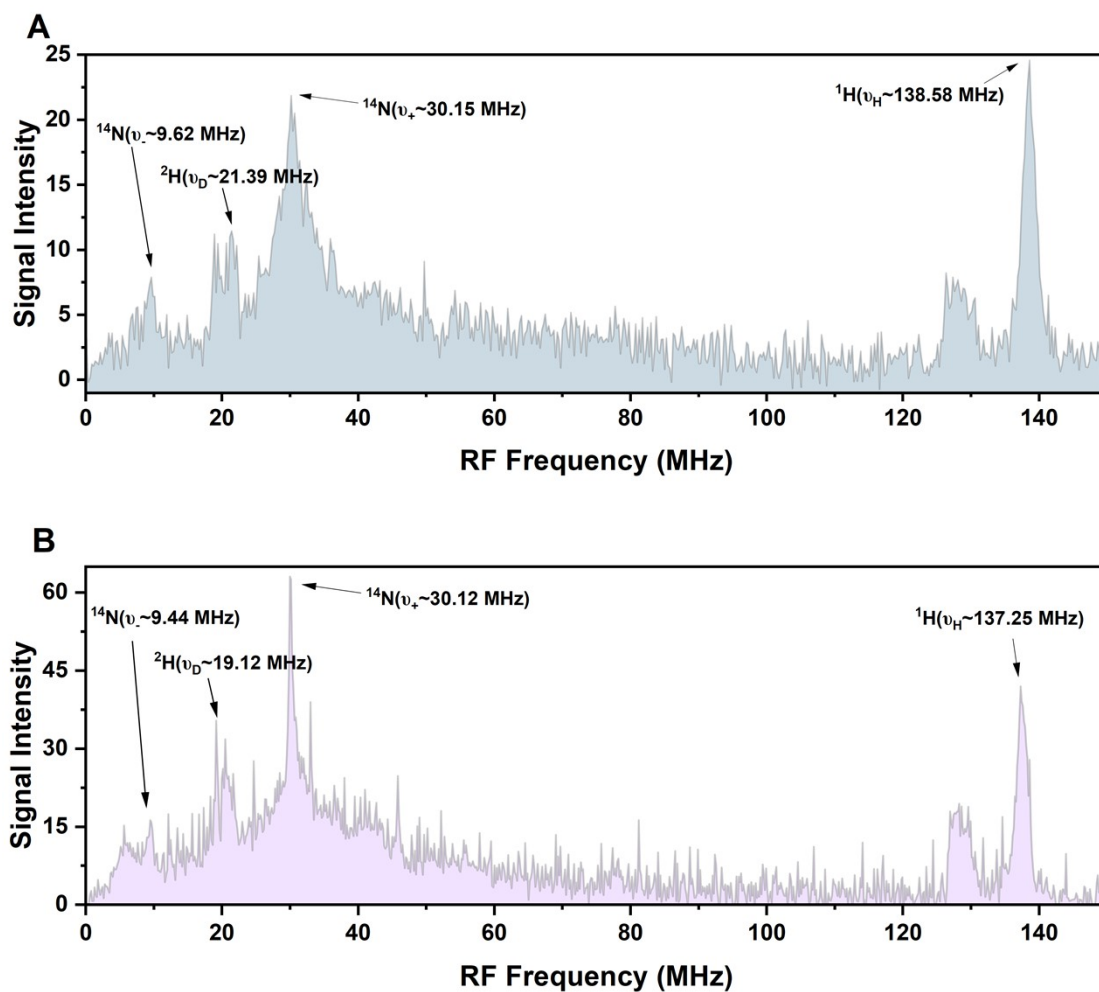


**Fig. S7** Preliminary W-band Davies ENDOR spectra of Cu(II)-APP<sub>142-172</sub> (A) and Cu(II)-APP<sub>145-170</sub> (B) recorded at 10 K. The spectra were obtained at the magnetic field setting corresponding to the maximum of the electron spin echo ( $g_{\perp}$  region).

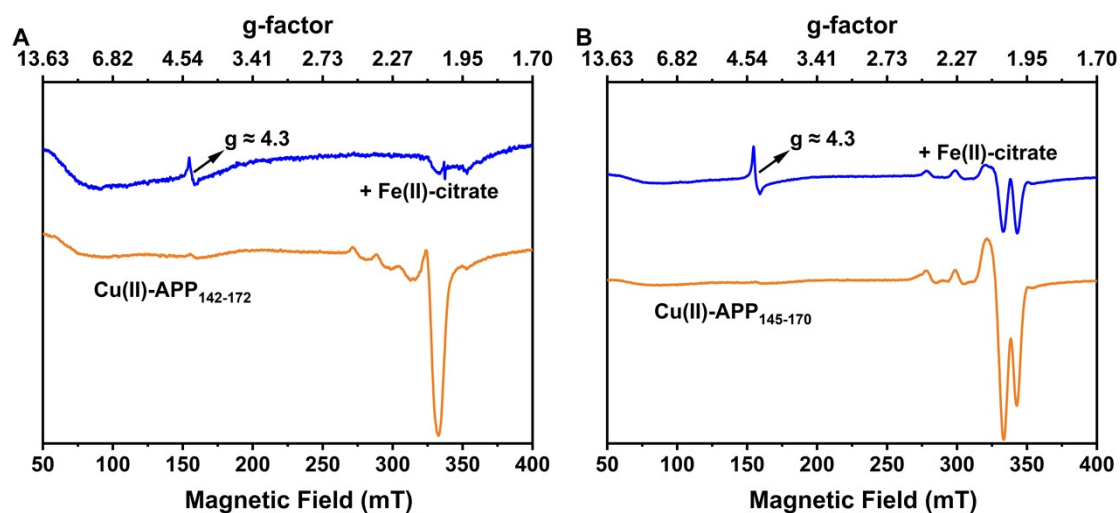


**Fig. S8** Fe(II)-citrate oxidation by Cu(II)-peptide complexes monitored by EPR spectroscopy under anaerobic conditions. (A) Cu(II)-APP<sub>142-172</sub> before (orange) and after (blue) addition of excess Fe(II)-citrate. The Cu(II) signal is effectively eliminated upon Fe(II)-citrate addition, consistent with reduction to EPR-silent Cu(I). The minor feature near  $g \approx 2.0$  in the blue trace of panel A originates from a light-induced resonator baseline distortion and is not sample-derived. (B) Cu(II)-APP<sub>145-170</sub> before (orange) and after (blue) Fe(II)-citrate addition. A residual Cu(II) contribution persists, indicating incomplete reduction in this system. The signal at  $g \approx 4.3$  in both panels is characteristic of high-spin Fe(III).